

RESEARCH

Open Access



# Thermo-amplifier circuit in probiotic *E. coli* for stringently temperature-controlled release of a novel antibiotic

Sourik Dey<sup>1</sup>, Carsten E. Seyfert<sup>2,3,4</sup>, Claudia Fink-Straube<sup>1</sup>, Andreas M. Kany<sup>2,3,4</sup>, Rolf Müller<sup>2,3,4</sup> and Shrikrishnan Sankaran<sup>1\*</sup>

## Abstract

Peptide drugs have seen rapid advancement in biopharmaceutical development, with over 80 candidates approved globally. Despite their therapeutic potential, the clinical translation of peptide drugs is hampered by challenges in production yields and stability. Engineered bacterial therapeutics is a unique approach being explored to overcome these issues by using bacteria to produce and deliver therapeutic compounds at the body site of use. A key advantage of this technology is the possibility to control drug delivery within the body in real time using genetic switches. However, the performance of such genetic switches suffers when used to control drugs that require post-translational modifications or are toxic to the host. In this study, these challenges were experienced when attempting to establish a thermal switch for the production of a ribosomally synthesized and post-translationally modified peptide antibiotic, darobactin, in probiotic *E. coli*. These challenges were overcome by developing a thermo-amplifier circuit that combined the thermal switch with a T7 RNA Polymerase. Due to the orthogonality of the Polymerase, this strategy overcame limitations imposed by the host transcriptional machinery. This circuit enabled production of pathogen-inhibitory levels of darobactin at 40 °C while maintaining leakiness below the detection limit at 37 °C. Furthermore, the thermo-amplifier circuit sustained gene expression beyond the thermal induction duration such that with only 2 h of induction, the bacteria were able to produce pathogen-inhibitory levels of darobactin. This performance was maintained even in physiologically relevant simulated conditions of the intestines that include bile salts and low nutrient levels.

**Keywords** Bacterial drug delivery, Probiotic, *E. coli* Nissle 1917, Darobactin, T7 RNA Polymerase, Thermo-amplifier, Anti-bacterial

\*Correspondence:

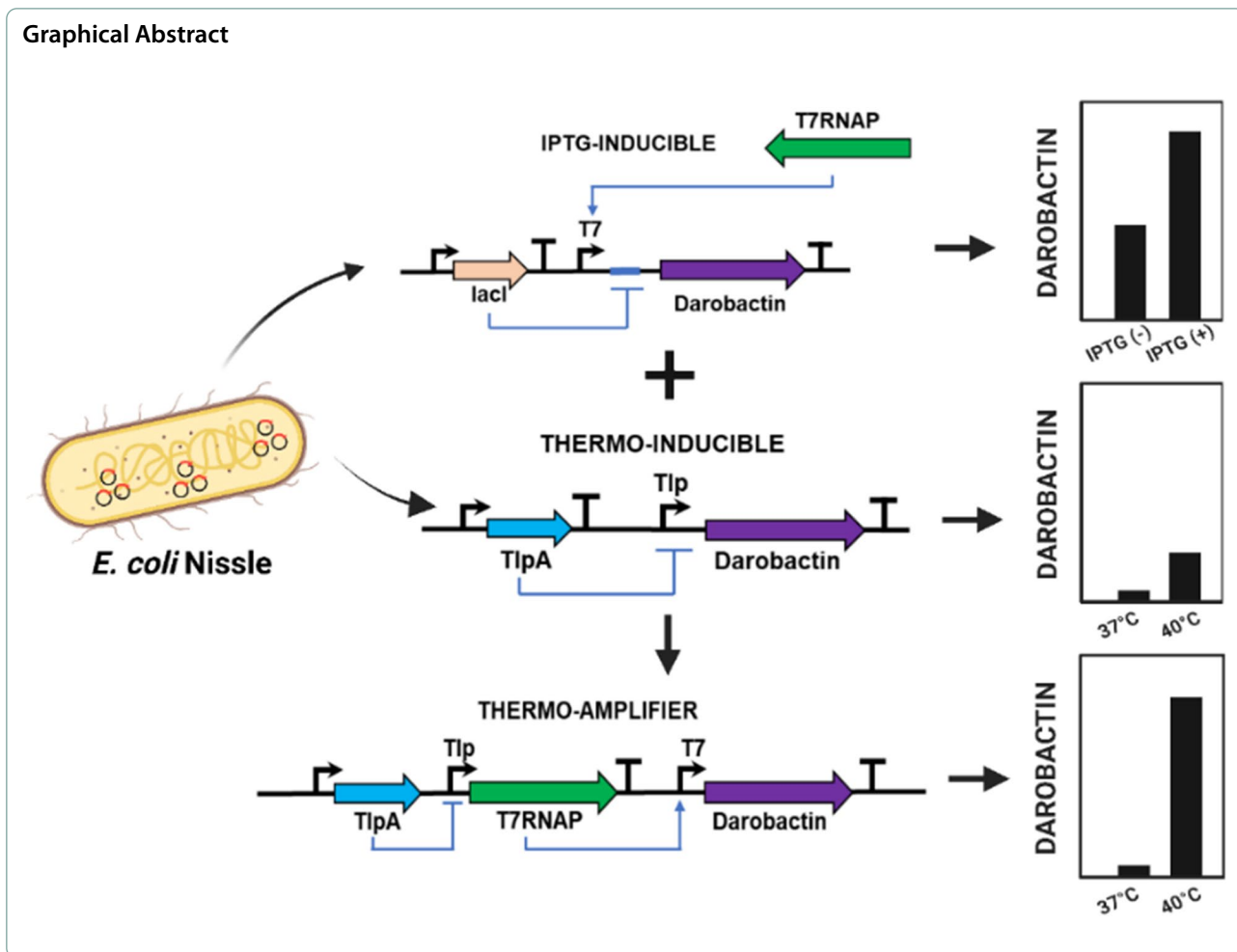
Shrikrishnan Sankaran

shrikrishnan.sankaran@leibniz-inm.de

Full list of author information is available at the end of the article



© The Author(s) 2024. **Open Access** This article is licensed under a Creative Commons Attribution 4.0 International License, which permits use, sharing, adaptation, distribution and reproduction in any medium or format, as long as you give appropriate credit to the original author(s) and the source, provide a link to the Creative Commons licence, and indicate if changes were made. The images or other third party material in this article are included in the article's Creative Commons licence, unless indicated otherwise in a credit line to the material. If material is not included in the article's Creative Commons licence and your intended use is not permitted by statutory regulation or exceeds the permitted use, you will need to obtain permission directly from the copyright holder. To view a copy of this licence, visit <http://creativecommons.org/licenses/by/4.0/>.



## Introduction

Among the growing spectrum of biopharmaceuticals, peptide drugs have experienced a rapid rise in development and clinical translation over the past decade with over 80 approved candidates worldwide [1, 2]. These intermediate-sized drugs, ranging from 500 Da to 5 kDa, offer strong and specific interactions with their intended targets while being amenable to chemical and microbial synthesis. Furthermore, peptides can be configured into an innumerable variety of functional structures through different amino acid combinations and post-translational modifications. To discover potent candidates from this vast set of possibilities various chemical, biomolecular and computational screening techniques have been employed [3]. Accordingly, peptide drugs have been developed to act as hormones, growth factors, neurotransmitters, protease-inhibitors, immune-modulators, ion channel ligands, and anti-infective agents [4]. Nevertheless, two major hurdles exist in the translation of peptide drugs to the clinics

– (i) achieving economically viable production yields, especially when their synthesis involves post-translational modifications, and (ii) limiting their instability in the body to deliver them in their active states to the disease site. A prominent example of a peptide drug facing these hurdles is darobactin, a novel antibiotic [5]. This antibiotic has shown potential in eliminating harmful Gram-negative pathogens, including highly virulent and antibiotic-resistant strains (ESKAPE classification) [5, 6]. The synthesis of darobactin is possible in *E. coli* and considerable efforts are underway to improve production yields for its economically viable upscaled manufacturing [7–9]. As a ribosomally synthesized and post-translationally modified peptide (RiPP), the darobactin operon includes the DarA peptide followed by DarBCDE enzymes that modify it into its active form and transport it out of the cell. Recombinant production of darobactin in *E. coli* currently provides the highest yields, although this is only up to 30 mg/L over 2 days [9]. Higher yields are desired since the half-life

of darobactin in the body is only 1 h, requiring the intraperitoneal administration of 50 mg darobactin per 1 kg of body weight in mice for demonstrating significant therapeutic efficacy [5]. Thus, for systemic administration in humans, the usage of several grams per day per individual is expected for treating bacterial infections with darobactin. However, darobactin's toxicity to the host *E. coli* plays a limiting role in improving production yields. In contrast, solutions offering localized delivery could alleviate the need for such high titers.

While several strategies are underway to improve production yields and stable delivery of peptide drugs like darobactin in the body, a unique “outside-the-box” approach for localized delivery is the development of engineered bacterial therapeutics [10–12]. This emerging technology involves the genetic programming of bacteria to synthesize and administer therapeutic substances within the body. The potential applications span a wide spectrum of medical conditions including infections, inflammatory disorders and cancer [13]. These engineered bacteria can produce and deliver peptide drugs directly in the body, thereby obviating the need to externally produce these drugs in high titers. Furthermore, they can be programmed with genetic switches to control the timing and dosage of drug release, thereby ensuring drug availability only when and where it is needed. This is particularly important for antimicrobial drugs, as their indiscriminate use is known to generate antibiotic-resistant microbes [14]. While most genetic switches are activated by chemical inducers like arabinose [15] or salicylate [16] that can be taken orally, switches responsive to physical stimuli like light [17] and heat [18] offer the advantage of rapid and local activation. In particular, thermo-responsive switches are highly attractive because they can be either self-activated under fever-like conditions or externally activated using non-invasive techniques, like focused ultrasound [19]. Through these unique possibilities, engineered bacterial therapeutics can achieve on-demand production of intricate and costly biopharmaceutical drugs directly at the required body-site, thus mitigating issues associated with stability during storage, transportation, and administration. By encapsulating such bacteria in biocompatible materials, it is also possible to create smart self-replenishing drug-delivery devices to treat chronic diseases [20–22]. Thus, engineered bacterial therapeutics offer the possibility to provide a tailored and patient-centric treatment approach.

However, when it comes to combining genetic switches with complex biosynthetic pathways, balancing stringent control in the OFF state with sufficient production for therapeutic efficacy in the ON state is a major challenge [23]. Achieving this balance often requires considerable

optimization of the genetic circuits and development of novel genetic modules [24]. In recent studies, promoter engineering enabled thermally regulated expression and release of oncolytic nanobodies [25] and tumor necrosis factor (TNF- $\alpha$ ) [26] from the probiotic *E. coli* Nissle 1917 strain for treating solid tumors in mice models. While these studies achieved activation of bacterial gene expression within the host, the output was limited to the production and secretion of a protein without post-translational modifications. In contrast only a few studies have addressed stimuli-responsive regulation of compounds produced through enzyme cascades [27, 28]. These studies often reveal that the regulated production of such compounds is more challenging compared to unmodified proteins due to greater leaky expression or lower output yields, especially when the product can be toxic to the host cell at high concentrations.

In this study, we address this challenge by engineering probiotic *E. coli* for thermo-switchable darobactin production (37 °C OFF, 40 °C ON). This approach avoids continuous release of the antibiotic from the engineered bacteria and activates it at temperatures associated with high fever. Notably, we faced the previously mentioned challenges of leaky and insufficient expression in different genetic circuits to achieve such switching. We were able to simultaneously resolve both issues by developing a genetic amplification strategy that resulted in a novel thermo-amplifier circuit with undetectable leakiness at 37 °C and darobactin production levels at 40 °C that inhibited the growth of the opportunistic pathogen *Pseudomonas aeruginosa* PAO1. Furthermore, we show that the thermo-amplifier circuit remains ON for several hours after only 2 h of heating, ensuring that its pathogen-killing activity can be triggered even with only a short duration of raised body temperature. Finally, the engineered strain was shown to maintain its ability to kill pathogens even in the presence of bile acids and under low-nutrient conditions that are expected to be encountered in the gastrointestinal tract. Thus, the thermo-amplifier circuit can be an efficient module to improve the performance of engineered bacterial therapeutics for the delivery of complex peptide drugs.

## Materials and methods

### Media, bacterial strains and growth conditions

Luria–Bertani (LB) growth media used for this study was procured from Carl-Roth GmbH, Germany. Unfractionated Bovine Bile (CAS No – 8008–63-7, B3883-25G) was purchased from Merck Millipore GmbH, Germany. NEB® 5-alpha Competent *E. coli* cells (C2987H) were routinely used for recombinant plasmid cloning and maintenance. The thermoamplifier constructs were assembled in chemically competent ABLE-K cells

(200,172) procured from Agilent Technologies (USA). ClearColi BL21 DE3 cells were obtained from BioCat GmbH (Heidelberg, Germany) and the alanine auxotrophic  $\Delta alr \Delta dadx$  ClearColi BL21 DE3 strain was created by Gen-H GmbH (Heidelberg, Germany) using Cre-loxP recombination technique. ClearColi were grown in LB broth supplemented with 2% (w/v) sodium chloride, with additional supplementation of 40  $\mu\text{g}/\text{mL}$  D-alanine for the  $\Delta alr \Delta dadx$  ClearColi strain. *E. coli* Nissle 1917 (EcN) was isolated from the commercially available Mutaflor<sup>®</sup> enteric coated hard capsules (Germany). *P. aeruginosa* PAO1 (DSMZ 22644) was obtained from DSMZ GmbH (Braunschweig, Germany).

#### Molecular biology reagents and oligonucleotides

Q5 DNA Polymerase was used for DNA amplification and colony PCR screening (New England Biolabs GmbH, Germany). Gibson Assembly and site-directed mutagenesis was performed using the NEBuilder HiFi DNA Assembly Cloning Kit (E5520S) and KLD Enzyme Mix (M0554S) respectively. Qiagen Plasmid Kit (12,125) was used for plasmid extraction and Wizard<sup>®</sup> SV Gel and PCR Clean-Up System (A9282) was used for DNA purification. Oligonucleotides used in this study were synthesized from Integrated DNA Technologies (Belgium) and recombinant plasmids were verified by Sanger Sequencing (Eurofins GmbH, Germany). The sequence annotated maps of the pTlp-DarA-AT and pTAMP-DarA-AT recombinant plasmids are listed in Fig. S8 and Fig. S9. The nucleotide sequences of the genetic modules tested in this study have been listed in Table S1.

#### Competent cell preparation

Electrocompetent cells of ClearColi and  $\Delta alr \Delta dadx$  ClearColi (alanine auxotroph) were prepared by repeated washing of bacterial pellet harvested at early exponential growth phase with 10% glycerol (v/v). Plasmids (500 ng) were transformed in the competent cells by electroporation at 1.8 kV, using 0.1 cm electroporation cuvettes (1,652,083) in the Bio-Rad Micropulser<sup>TM</sup> Electroporator. To prepare chemically competent EcN and EcN-T7 cells, bacterial cultures were grown overnight in LB broth at 37 °C, 250 rpm and subcultured in 100 mL of fresh LB media [1:100 (v/v) dilution]. The cultures were incubated at 37 °C, 250 rpm until an  $\text{OD}_{600}=0.4$  was reached. The bacteria were pelleted down by centrifugation at 4000 rpm (3363 X g), 4 °C for 15 min and the supernatant was discarded. The bacterial pellet was then washed twice with ice-cold  $\text{CaCl}_2$  (200 mM) and once with a 1:1 mixture of  $\text{CaCl}_2$  (200 mM) and glycerol (10% w/v). After the final wash, the pellet was resuspended in 1 mL of

$\text{CaCl}_2$  + glycerol mixture and stored at -80 °C as 100  $\mu\text{L}$  aliquots. For bacterial transformation, 1  $\mu\text{g}$  of the plasmids were added to the competent cells and gently mixed by flicking. The competent cells were then chilled on ice for 30 min and transferred to a 42 °C water bath for 45 s, followed by incubation on ice for 2 min. SOC media (900  $\mu\text{L}$ ) was added and mixed, and the cell suspension was incubated at 37 °C, 250 rpm for an hour before plating on LB agar with appropriate antibiotics.

#### Inducible mCherry protein production

Recombinant ClearColi BL21 DE3 strains (pNOSO-mCherry and pUC-Tlp-mCherry) were inoculated in LB-NaCl media and cultivated overnight at 30 °C, 250 rpm with appropriate antibiotics. Following day, both the bacterial suspensions were subcultured in 25 mL of fresh Formulated Media (FM) [Composition:-  $\text{K}_2\text{HPO}_4$  – 12.54 g/L,  $\text{KH}_2\text{PO}_4$  – 2.31 g/L, D-Glucose – 4 g/L,  $\text{NH}_4\text{Cl}$  – 1 g/L, Yeast Extract – 12 g/L, NaCl – 5 g/L,  $\text{MgSO}_4$  – 0.24 g/L] in a sterile glass conical flask (250 mL) at a 1:25 (v/v) ratio and incubated at 37 °C, 250 rpm. Once the bacterial samples reached an  $\text{OD}_{600}$  of 0.4, 500  $\mu\text{M}$  of IPTG was added to the pNOSO-mCherry culture, and the pUC-Tlp-mCherry culture was shifted to 40 °C for further incubation. Controls were included for both strains as non-IPTG supplemented samples (pNOSO-mCherry, 37 °C) and non-temperature elevated samples (pUC-Tlp-mCherry, 37 °C). Post 24 h incubation, the  $\text{OD}_{600}$  of all the cultures was determined using the NanoDrop Microvolume UV–Vis Spectrophotometer (ThermoFisher Scientific GmbH, Germany). 1 mL of each bacterial culture was normalized to  $\text{OD}_{600}$  of 0.8 to maintain an equivalent cell count. The normalized cultures were centrifuged at 13,000 rpm (16200Xg) and washed thrice with sterile Dulbecco's 1×PBS (Phosphate Buffer Saline) solution. 200  $\mu\text{L}$  of the resuspended bacterial cultures were transferred to a clear bottom 96-well microtiter plate (Corning<sup>®</sup> 96 well clear bottom black plate, USA). The absorbance (600 nm wavelength) and mCherry fluorescence intensity ( $\text{Ex}_\lambda / \text{Em}_\lambda=587 \text{ nm}/625 \text{ nm}$ ) of the respective bacterial samples were then measured in the Microplate Reader Infinite 200 Pro (Tecan Deutschland GmbH, Germany). The z-position and gain settings for recording the mCherry fluorescent intensity were set to 19,442  $\mu\text{m}$  and 136 respectively. Fluorescence values were normalized with the optical density of the bacterial cells to calculate the Relative Fluorescence Units (RFU) using the formula  $\text{RFU} = \text{Fluorescence}/\text{OD}_{600}$ . For determining fold change, the following formula was used =  $\text{RFU} (\text{induced culture})/\text{RFU} (\text{uninduced culture})$ .

### Production and purification of darobactin A

The production and purification of darobactin A was performed as described previously for darobactin D [29].

### Cultivation of the darobactin production strains

Recombinant strains were inoculated into LB (for EcN and EcN-T7 variants) and LB-NaCl (for ClearColi BL21 DE3 variants) from the glycerol stocks and cultivated overnight at 30 °C, 250 rpm with appropriate antibiotics. The bacterial suspensions were then subcultured in 25 mL of fresh Formulated Media (FM) in a sterile glass conical flask (250 mL) at a 1:25 (v/v) ratio. The samples were kept at temperatures 37 °C and 40 °C for different temporal periods. For IPTG inducible conditions, 500 µM IPTG was added to the cultures at  $OD_{600}=0.4$ . Bacterial growth curve was obtained by measuring  $OD_{600}$  at different time intervals using the Microplate Reader Infinite 200 Pro.

### Electrospray ionization—mass spectrometry (ESI-MS) based darobactin quantification

For Figs. 1B, D, 2B, D, 4D, and 5A, C, S2B, S3A and S3B the following method was used: LC/ESI QTOF-MS analysis is performed on a 1260 Infinity LC in combination with a 6545A high-resolution time-of-flight mass analyzer, both from Agilent Technologies (Santa Barbara, CA, USA). Separation of 1 µl of sample is performed using a Poroshell HPH-C18 column (3.0×50 mm, 2.7 µm) equipped with the same guard column (3.0×5 mm, 2.7 µm) by a linear gradient from (A) ACN+0.1% formic acid to (B) water+0.1% formic acid at a flow rate of 500 µl/min and a column temperature of 45 °C. Gradient conditions are as follows: 0–0.5 min, 95% B; 0.5–6 min, 95–60.5% B; 6–9.5 min 60.5–20% B at 1500 µl/min (column cleaning), 9.5–13 min 95% B down to 500 µl/min (equilibrium).

After separation, the LC flow enters the dual AJS ESI source set to 3500 V as capillary voltage, 40 psi nebulizer gas pressure and 7 l/min dry gas flow, and 300 °C dry gas temperature. The TOF parameters used are high resolution mode (4 GHz), 140 V fragmentor and 45 V skimmer voltage. The mass spectra are acquired in the time interval of 2–6 min in full scan mode in the range  $m/z$  150–3000 with a spectra rate of 4/s. For quantification of the darobactin, the positive charged mass  $[M+2H]_2^+$  at  $m/z$  483.7089 Da were extracted and automatically integrated using Mass Hunter software. Standards were prepared from darobactin stock solution of 100 µg/ml in mobile phase (5%A, 95%B) or blank media. Calibration was done between 0 and 1 µg/ml or 0 and 10 µg/ml with recovery rates 97–105%.

For the data in Fig. 3B and C, the following method was used: darobactin was quantified using a Vanquish Flex

UHPLC (Thermo Fisher, Dreieich, Germany), coupled to a TSQ Altis Plus mass spectrometer (Thermo Fisher, Dreieich, Germany). Samples were diluted 1:10 in PBS pH 7.4, followed by addition of 2 volumes 10%MeOH/ACN containing 15 nM diphenhydramine as internal standard. Samples were centrifuged (15 min, 4 °C, 4000 rpm) before analysis and darobactin content quantified in SRM mode using a calibration curve up to 5 µM. LC conditions were as follows: column: Hypersil GOLD C-18 (1.9 µm, 100×2.1 mm; Thermo Fisher, Dreieich, Germany); temperature 40 °C; flow rate 0.700 ml/min; solvent A: water+0.1% formic acid; solvent B: acetonitrile+0.1% formic acid; gradient: 0–0.2 min 10% B, 0.2–1.2 min 10–90% B, 1.2–1.6 min 90% B, 1.6–2.0 min 10% B. MS conditions were as follows: vaporizer temperature 350 °C, ion transfer tube temperature 380 °C, Sheath Gas 30, Aux Gas 10, Sweep Gas 2; spray voltage: 4345 V, mass transition: 483.75 – 475.083 ( $[M+2H]_2^+$ ), collision energy: 11.0 V; Tube lens offset 55 V.

For analyzing experimental samples, the bacterial biomass was removed post-incubation by centrifugation [4000 rpm (3363Xg), 30 min, 4 °C] and the respective supernatants were filter-sterilized with 0.22 µm filters (Carl Roth, Germany) before proceeding with ESI-MS analysis along with their respective blank controls.

### qPCR analysis for plasmid retention

Bacterial cultures were cultivated in 5 mL of LB media (supplemented with 100 µg/mL ampicillin) at 30 °C with continuous shaking (250 rpm). The following day, the bacterial suspension was subcultured in 25 mL of FM both with and without antibiotic supplementation (100 µg/mL ampicillin) in a 1:25 (v/v) ratio. Bacterial cultures were immediately kept at 40 °C and incubated for 24 h. Post 24 h incubation, the  $OD_{600}$  was measured, and fresh FM cultures were inoculated with the respective bacterial cultures at a starting  $OD_{600}$  of 0.01. This procedure was repeated over 5 days, resulting in ~50 consecutive bacterial generations.

For qPCR analysis, 1 mL of the bacterial samples after every 10 generations were normalized to an  $OD_{600}$  of 0.8 with sterile PBS. The normalized cultures were centrifuged at 13,000 rpm (16200Xg) and washed thrice with sterile Dulbecco's 1×PBS solution. 500 µl of the bacterial samples were then kept at 98 °C for 15 min to undergo lysis in a static thermomixer (Eppendorf GmbH, Germany) according to the reported protocol [30]. The samples were then stored at -20 °C for further analysis. Post collection of these bacterial samples till 50 generations, qPCR was performed using the iTaq™ Universal SYBR® Green Supermix (BioRad GmbH, Germany) in the Bio-Rad CFX96 Real time system C1000 Touch thermal cycler. To prevent sample heterogeneity, qPCR

reactions were conducted with primers specific to the pUC replication origin of the recombinant plasmid. The nucleotide sequences of the qPCR primers used are listed in Table S2. The quantification curve (Cq) values were selected by the regression determination mode and the mean  $\Delta Cq$  was determined by the following formula:  $\Delta Cq = Cq$  (50th generation) –  $Cq$  (10th generation). The data were finally represented in the form of fold change calculated as: Mean  $\Delta Cq$  (With Ampicillin)/Mean  $\Delta Cq$  (Without Ampicillin).

#### qRT-PCR analysis for gene expression

Bacterial cultures were cultivated in 5 mL of LB media (supplemented with 100  $\mu\text{g/mL}$  ampicillin) at 30 °C with continuous shaking (250 rpm). The following day, the bacterial suspension was subcultured in 25 mL of non-antibiotic supplemented FM in a 1:25 (v/v) ratio. Post 6 h incubation at the respective temperatures, the  $OD_{600}$  was determined using the NanoDrop Microvolume UV–Vis Spectrophotometer (ThermoFisher Scientific GmbH, Germany). All the bacterial cultures were normalized to  $OD_{600}$  of 0.8 to maintain an equivalent cell count. The normalized cultures were centrifuged at 13,000 rpm (16200Xg) and washed thrice with sterile Dulbecco's 1 $\times$  PBS solution. The bacterial pellet was then resuspended in 1X DNA/RNA protection reagent supplied with the Monarch Total RNA Miniprep Kit (NEB #T2010) (New England BioLabs GmbH, Germany) and subjected to mechanical lysis using the FastPrep-24™ 5G bead beating grinder system (MP Biomedicals Germany GmbH, Germany). Total RNA was isolated according to the manufacturer guidelines and measured at 260 nm to determine the net yield and purity. 500 ng of the total RNA from all extracted samples were then immediately converted into cDNA using the Thermo-Scientific Revertaid first strand cDNA synthesis kit (#K1622). Real time qPCR was performed using the iTaq™ Universal SYBR® Green Supermix (BioRad GmbH, Germany) in the Bio-Rad CFX96 Real time system C1000 Touch thermal cycler to determine the gene expression level of target genes. Bacterial 16S rRNA levels were also measured for all the samples as a control [31]. The specific sequences of qRT-PCR primers are listed in Table S2. The quantification curve (Cq) values were selected by the regression determination mode and the mean  $\Delta Cq$  values were determined by the following formula:  $-\Delta Cq = Cq$  (37 °C) –  $Cq$  (40 °C). The data were finally represented in the form of fold change calculated as  $2^{\Delta Cq}$ .

#### *P. aeruginosa* PAO1 survival assay

*P. aeruginosa* PAO1 was inoculated into 5 mL FM from glycerol stock and subjected to overnight incubation at 37 °C with 230 rpm orbital shaking. The following

day, *P. aeruginosa* PAO1 was subcultured in fresh FM at 1:50 ratio (v/v) and grown till it reached log phase ( $OD_{600} = 0.4$ ). The log-phase bacteria were further diluted in FM to optimize the bacterial cell number to  $55 \times 10^5$  CFU/mL. 10  $\mu\text{L}$  of diluted bacterial culture were added to 100  $\mu\text{L}$  of filter-sterilized supernatants (mentioned above) in a sterile 96-well U-bottom transparent plate (REF 351177, Corning, USA) to bring the final bacterial cell number to  $5 \times 10^5$  CFU/mL. The plates were incubated under static conditions for 18 h at 37 °C and bacterial growth was determined by measuring absorbance at 600 nm in Microplate Reader Infinite 200 Pro.

#### Darobactin production in nutrient-limited media

Bacterial cultures were cultivated overnight in 5 mL of LB media (supplemented with 100  $\mu\text{g/mL}$  ampicillin) at 30 °C with continuous shaking (250 rpm). The following day, the bacterial suspension was subcultured in 25 mL of FM (without antibiotic supplementation) in a 1:25 (v/v) ratio and incubated at 30 °C for 24 h. Post incubation, the bacterial pellet was centrifuged at 4000 rpm (3363Xg), for 50 min, 4 °C and the supernatant was discarded. The bacterial pellet was then resuspended in 25 mL of M9 Minimal Media [ $\text{Na}_2\text{HPO}_4 \cdot 7\text{H}_2\text{O}$  – 12.8 g/L,  $\text{KH}_2\text{PO}_4$  – 3 g/L,  $\text{NH}_4\text{Cl}$  – 1 g/L, NaCl – 0.5 g/L, D-Glucose – 4 g/L,  $\text{MgSO}_4$  – 0.24 g/L,  $\text{CaCl}_2$  – 0.011 g/L] and maintained at different incubation temperatures for 6 h. For the bile tolerance test, the bacterial pellet was resuspended in M9 Minimal Media supplemented with 0.3% (w/v) Bovine Bile [32], filter sterilized using a 50 mL Nalgene™ Rapid-Flow™ Sterile Disposable 0.22  $\mu\text{m}$  Filtration Device (Catalog Number 564–0020, ThermoFisher Scientific GmbH, Germany). Post incubation, the bacterial pellet was centrifuged and discarded, whereas the filter-sterilized supernatant was further assessed for the overall darobactin concentration and its antimicrobial activity against *P. aeruginosa* PAO1.

## Results

### Functional characterization of inducible darobactin production

At first, an endotoxin-free *E. coli* strain, ClearColi BL21 DE3 [33], was engineered to produce and secrete darobactin by transforming it with the pNOSO-darABCDE plasmid [9]. This *E. coli* strain was selected based on our previous experience in engineering it for living therapeutic applications [27, 34, 35]. In the pNOSO-darABCDE plasmid, the DarA propeptide is encoded downstream of an IPTG-inducible T7-lacO promoter-operator complex and the DarBCDE enzyme cascade is constitutively expressed (Fig. 1A). As highlighted by Groß and coworkers before, *darBCD* encode for a permease protein (DarB), membrane fusion protein (DarC)

and ATP-binding protein (DarD), all together comprising a tripartite efflux pump facilitating darobactin export from the bacterial chassis. The DarE protein is a radical S-adenosyl-L-methionine (SAM) enzyme which catalyzes the formation of the ether and C–C crosslinking in the heptapeptide core structure ( $W^1-N^2-W^3-S^4-K^5-S^6-F^7$ ) of the DarA propeptide [36]. This plasmid was cloned in ClearColi BL21 DE3, since this strain has been mutated to be endotoxin-free, thereby making it more immune-compatible than the regular BL21 DE3 strain that expresses the T7 RNA Polymerase (T7-RNAP) needed for recombinant gene expression. The darobactin amount secreted by this strain in Formulated Medium (FM) at 37 °C following 24 h of IPTG induction (500  $\mu$ M) was  $\sim 2.5$   $\mu$ g/mL, detected directly in the medium by Electrospray ionization–mass spectrometry (ESI–MS). This corresponded to the previously reported minimum inhibitory concentrations (MIC) determined for the commonly tested model pathogenic strain, *P. aeruginosa* PAO1 ( $> 2$   $\mu$ g/mL) [5]. However, even without IPTG induction, the system was considerably leaky and produced  $\sim 1$   $\mu$ g/mL of darobactin in FM (Fig. 1B).

To achieve thermoresponsive production and secretion of darobactin, its biosynthetic gene cluster (BGC) was cloned into the thermogenetic pTlpA39-mWasabi

plasmid (#Addgene 86116). In this system, a thermosensitive repressor (TSR) undergoes dimerization and represses the  $P_{tlpA}$  promoter at temperatures below 39 °C. Above this threshold temperature, the repressor reverts to its monomeric state allowing  $P_{tlpA}$  promoter-based gene expression [18]. For the thermally activated constructs, *darA* was encoded downstream of the  $P_{tlpA}$  promoter, whereas the DarBCDE enzyme cascade was constitutively expressed by the promoter  $P_{TN5}$  as in the pNOSO-darABCDE plasmid. Notably, the pNOSO vector backbone has a medium-copy number p15A replicon, whereas the pTlpA39 plasmid is based on a high-copy number pMB1 replicon (pUC). Thus, two plasmids encoding thermoresponsive darobactin production modules were constructed with each of these replicons and annotated as p15A-Tlp-DarA and pUC-Tlp-DarA respectively (Fig. 1C). While no darobactin was detected in the culture medium of p15A-Tlp-DarA ClearColi strain after 24 h incubation (at both 37 °C and 40 °C), the ClearColi strain containing pUC-Tlp-DarA released detectable levels of darobactin in the culture medium at both incubation temperatures. The resulting darobactin concentration in the medium for the pUC-Tlp-DarA ClearColi strain at 40 °C ( $\sim 0.13$   $\mu$ g/mL) was  $\sim 4\times$  fold higher than that observed at 37 °C ( $\sim 0.03$   $\mu$ g/mL) (Fig. 1D). Although

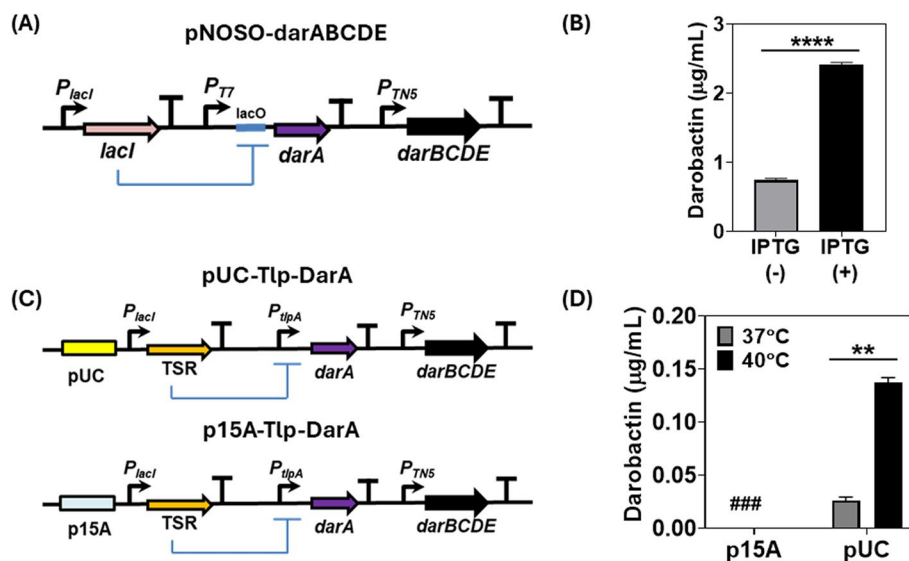


**Fig. 1** Comparative analysis of Darobactin production by inducible genetic circuit modules. **A** Schematic representation of the pNOSO-darABCDE gene circuit **(B)** Darobactin concentration in the liquid medium ( $\mu$ g/mL) for the pNOSO-darABCDE construct in ClearColi BL21 DE3 strain after 24 h of incubation. The bacteria were induced with 500  $\mu$ M of IPTG at  $OD_{600} = 0.4$  in Formulated Media (FM) supplemented with 50  $\mu$ g/mL kanamycin. The error bars represent standard deviation based on three independent measurements (\*\*\*\* $p < 0.0001$  as calculated by paired t-test) **(C)** Schematic representation of the thermoresponsive darobactin gene circuits based on high—copy (pUC-Tlp-DarA) and medium-copy (p15A-Tlp-DarA) number replication origin. The thermosensitive repressor (TSR) represses  $P_{tlpA}$  promoter at physiological temperature (37 °C) and is derepressed at temperatures beyond  $> 39$  °C **(D)** Darobactin concentration in the liquid medium ( $\mu$ g/mL) for the p15A and pUC origin based Tlp-DarA gene circuits in ClearColi BL21 DE3 strains after 24 h of incubation at 37 °C and 40 °C. (###) represents darobactin concentration lower than the Limit of Detection (LOD) by ESI–MS. The error bars represent standard deviation based on three independent measurements (\*\* $p = 0.0016$  as calculated by paired t-test)

the darobactin concentrations were significantly lower than the desired MIC for inhibiting Gram-negative pathogenic strains, thermoresponsive production was confirmed. This encouraged us to optimize the performance of the gene circuit based on the high-copy number plasmid, pUC-Tlp-DarA.

To further determine the expression strength and fold-change of the inducible promoters, the *darA* was replaced by a red fluorescent reporter gene (*mCherry*) in the pNOSO and pUC-Tlp vector backbones without altering any other coding sequence (CDS) to create the pNOSO-mCherry (Fig. S1A) and pUC-Tlp-mCherry (Fig. S1B) constructs, respectively. Post IPTG induction, it was observed that mCherry production for the pNOSO-mCherry ( $P_{T7}$  promoter) strain was only  $\sim 2.5\times$  fold higher than the uninduced control (Fig. S1C). On the other hand, the pUC-Tlp-mCherry ( $P_{tlpA}$  promoter) strain had a  $\sim 40\times$  fold increase in fluorescence at 40 °C compared to 37 °C (Fig. S1D). In addition to the superior fold change, the pUC-Tlp-DarA circuit also exhibited stronger mCherry production [in terms of relative fluorescence unit (RFU)] at 40 °C (Fig. S1F) than the IPTG induced pNOSO-mCherry circuit (Fig. S1E). However, this contrasting trend between the darobactin and mCherry production by the same pUC-Tlp based recombinant plasmids suggested that the genetic circuits encoding darobactin production might be influenced by alternate factors like the *darA:darE* transcript ratio [8] or intracellular toxicity [29], rather than the production rate of DarA alone. In accordance with our observations regarding pNOSO-darABCDE, there was considerable basal level expression of mCherry observed for pNOSO-mCherry samples grown without any IPTG supplementation. On the other hand, mCherry expression was tightly regulated by the TSR protein in pUC-Tlp-mCherry samples at 37 °C in line with our previous report [37]. This shows that TSR protein-based gene regulation is more effective than the conventional lacI repressor protein which is known for its inability to mediate strong repression [38].

Another major factor that distinguishes darobactin production from that of mCherry is that darobactin could exert a detrimental effect on the growth of the bacterial host [5, 9]. To validate this hypothesis, constitutive expression of darobactin was tested in ClearColi by exchanging the thermoresponsive elements in pUC-Tlp-DarA with the  $P_{T7}$  promoter (pT7-DarA), placed directly upstream of the *darA* gene for driving its constitutive transcription by the cognate T7-RNAP genomically encoded in ClearColi. As expected, this caused a significant reduction in the bacterial biomass ( $\sim 100$  mg per 25 mL of liquid culture) in comparison to the IPTG-induced pNOSO-darABCDE construct ( $\sim 430$  mg per

25 mL of liquid culture) when cultivated at 37 °C for 24 h (Fig. S2A). A considerable reduction in the overall darobactin concentration ( $\sim 0.09$   $\mu\text{g/mL}$ ) was also observed for the pT7-DarA ClearColi strain when compared to the IPTG-induced pNOSO-darABCDE ClearColi strain (Fig. S2B). It could be deduced that the constitutive expression of darobactin by the pT7-DarA construct affected the growth of the producer strain and in-turn the darobactin production levels. Therefore, inducible expression of darobactin was essential to achieve higher darobactin concentration without compromising growth of the microbial chassis.

### Selection of an efficient antibiotic supplementation-free plasmid retention strategy

Before further optimization of thermoresponsive darobactin production, strategies to retain the pUC-Tlp-DarA plasmid in an antibiotic-free manner were tested. Earlier reports on engineered probiotics have highlighted the importance of maintaining the genetic stability of the heterologous protein-encoding genes during bacterial growth [39]. Although genetic stability can be achieved by integrating the heterologous genes in the host genome, studies have shown that this could significantly reduce the overall production [40] and secretion [41] levels of recombinant proteins. As we were unable to observe darobactin production in the liquid cultures using a medium-copy number replication origin (p15A ori), we decided not to proceed with genomic integration of the recombinant genetic modules for this study. As low but detectable levels of darobactin were observed for the thermoresponsive genetic circuit based on the high-copy number pUC replication origin, we chose this recombinant construct for assessing the two commonly employed plasmid retention strategies based on nutrient auxotrophy [42] and toxin-antitoxin dependent post-segregational killing [43]. For auxotrophy based plasmid retention, the alanine racemase genes (*alr* and *dadX*) essential for D-alanine biosynthesis in ClearColi were deleted from the bacterial genome. The resultant double knockout  $\Delta alr \Delta dadX$  ClearColi strain could therefore only be cultivated when the growth medium was supplemented with D-alanine. The *alr* gene with its native promoter was then amplified from *E. coli* DH5 $\alpha$  genomic DNA and cloned into the vector backbone of pUC-Tlp-DarA to create the pTlp-DarA-*alr* construct (Fig. 2A). Once transformed with this recombinant plasmid, the constitutive expression of the *alr* gene could then sustain the growth of the  $\Delta alr \Delta dadX$  ClearColi strain even in the absence of D-alanine supplementation and support plasmid retention. For the toxin-antitoxin (TA) based plasmid retention strategy, a type II TA gene pair, *txe-axe*, originally isolated from *Enterococcus faecium*

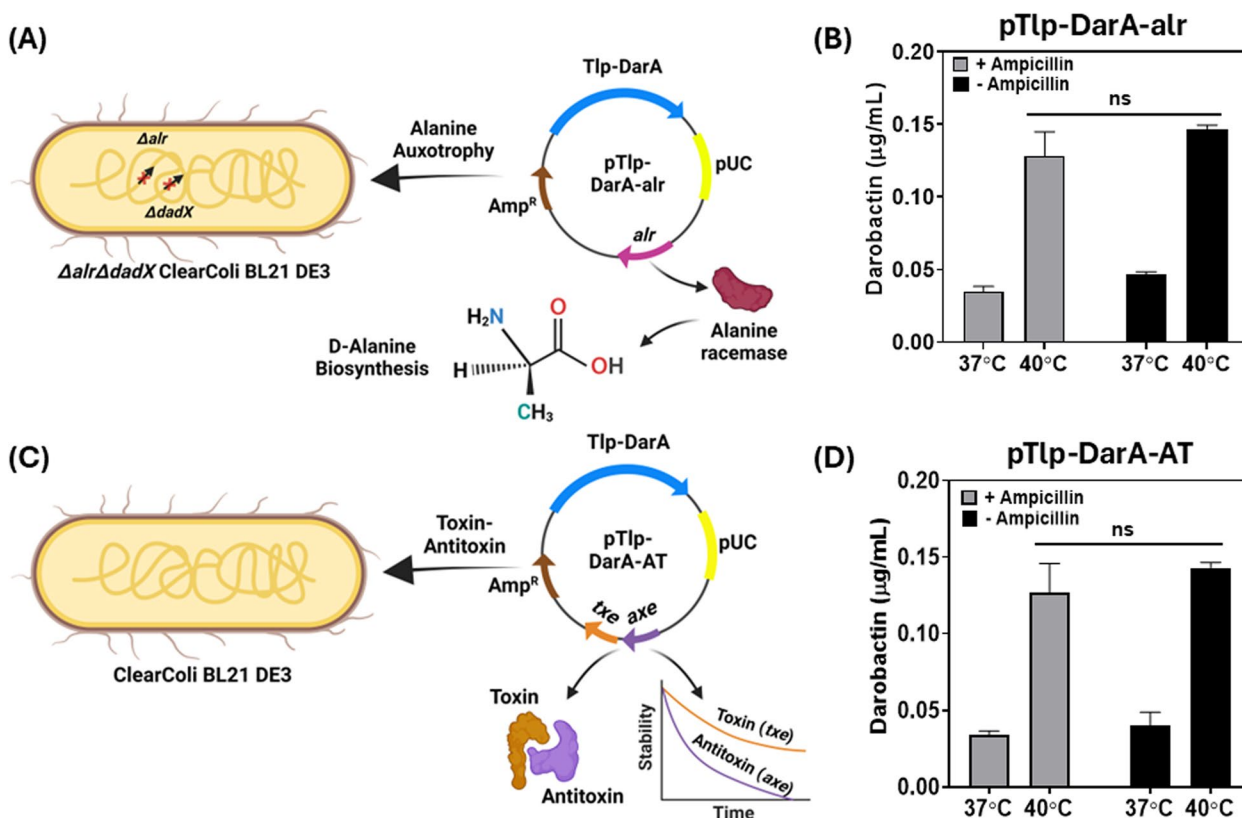


**Fig. 2** Testing the performance of plasmid retention modules without antibiotic supplementation. **A** Schematic representation of the pTlp-DarA-alsr construct transformed in  $\Delta alr \Delta dadX$  ClearColi BL21 DE3 strain. The integration of the alanine racemase (*alsr*) gene in the pUC-Tlp-DarA vector backbone facilitates alanine racemase-based conversion of L-alanine to D-alanine, responsible for bacterial cell wall synthesis in the auxotrophic strain **(B)** Darobactin concentration ( $\mu\text{g/mL}$ ) in the liquid medium for the pTlp-DarA-alsr construct after 24 h of incubation at 37 °C and 40 °C, both with and without ampicillin (100  $\mu\text{g/mL}$ ) supplementation. The error bars represent the standard deviation based on three independent measurements ( $^{ns}p=0.1482$  as calculated by paired t-test) **(C)** Schematic representation of the pTlp-DarA-AT construct transformed in ClearColi BL21 DE3 strain. The integration of the *txe-axe* toxin—antitoxin (TA) gene pair in the pUC-Tlp-DarA vector backbone mediates plasmid retention by its endoribonuclease activity and differential protein stability rates **(D)** Darobactin concentration ( $\mu\text{g/mL}$ ) in the liquid medium for the pTlp-DarA-AT construct after 24 h of incubation at 37 °C and 40 °C, both with and without ampicillin (100  $\mu\text{g/mL}$ ) supplementation. The error bars represent the standard deviation based on three independent measurements ( $^{ns}p=0.2584$  as calculated by paired t-test)

was used [44]. Once the Txe endoribonuclease protein is expressed, it is actively bound by its less stable counterpart, the Axe antitoxin protein, thereby preventing it from targeting the intracellular RNA population. However, if the recombinant strain loses the *txe-axe* gene-harboring plasmid, a drastic decline in Axe antitoxin concentration releases the Txe endoribonuclease, causing spontaneous RNA cleavage and bacterial growth arrest [45]. Recent studies have shown that incorporating the *txe-axe* TA module in the recombinant constructs allowed stable plasmid retention in *E. coli* over several generations, both under *in-vitro* [46] and *in-vivo* conditions [47]. The *txe-axe* gene pair was amplified from the pUC-GFP-AT (Addgene #133,306) plasmid and cloned into pUC-Tlp-DarA to create the pTlp-DarA-AT plasmid (Fig. 2C). The antibiotic supplementation-free retention plasmids, pTlp-DarA-alsr and pTlp-DarA-AT, were transformed in

$\Delta alr \Delta dadX$  ClearColi and unmodified ClearColi strains, respectively and cultivated in FM for 24 h, both with and without antibiotic supplementation (100  $\mu\text{g/mL}$  ampicillin). Post incubation, no significant difference of darobactin concentrations (liquid medium) was observed for the strains containing either pTlp-DarA-alsr (Fig. 2B) or pTlp-DarA-AT (Fig. 2D) in the absence of the antibiotic when compared to in the presence of it. The fold change (~4x) in darobactin production in response to the incubation temperatures also remained unaffected during this period. These results suggested that both approaches could effectively retain the engineered plasmids during bacterial growth and simultaneous darobactin production for 24 h even in the absence of antibiotic supplementation. As no distinct advantage of either strategy was noticed in terms of darobactin production in the tested temporal period, preference was given to the *txe-axe* TA

system for its ability to be used across several related *E. coli* strains without them having to undergo any permanent genomic modifications [25].

### Optimized genetic circuit to increase darobactin production

From the previous results, it was determined that the  $P_{T7}$  promoter with the cognate T7-RNAP was able to support high levels of darobactin production but poor inducible fold-changes. On the other hand, the  $P_{tlpA}$  promoter along with its TSR was found to mediate thermoresponsive darobactin production with an appreciable fold change between 37 °C and 40 °C but poor overall concentration in the liquid medium. Therefore, to obtain a higher darobactin concentration while maintaining thermoresponsive production, we decided to combine components of both inducible systems to design a thermo-amplifier circuit (pTAMP). In this genetic circuit, *darA* gene expression is mediated by the  $P_{T7}$  promoter and the production of its cognate T7-RNAP [amplified from the mBP-T7-RNAP plasmid (Addgene #74,096)] is controlled by the TSR regulated  $P_{tlpA}$  promoter (Fig. 3A). Notably, such a circuit could not be tested in ClearColi,

since the constitutively expressed *t7-RNAP* gene integrated into the bacterial genome would interfere with the performance of the recombinant circuit. Thus, as an alternative, we chose the probiotic EcN strain for testing the performance of the recombinant plasmid because of its prior use as a living therapeutic agent [48]. However, before proceeding with the testing of the pTAMP circuit we needed to assess whether darobactin production could be sustained by the EcN strain. For that, we first transformed the pNOSO-darABCDE plasmid in the EcN-T7 strain (DSMZ 115365), an engineered EcN variant with a genomic integration of the constitutively expressed *t7-RNAP* gene [49]. Post IPTG induction, the darobactin levels obtained from this recombinant EcN-T7 strain after 24 h in FM was over 3x-fold higher (~8.15 µg/mL) than that from the ClearColi strain. This suggested that  $P_{T7}$  driven production of darobactin could also be sustained in EcN without compromising the metabolic fitness of the microbial chassis. Furthermore, similar to what was observed with the pNOSO-darABCDE ClearColi strain, the corresponding EcN-T7 strain also exhibited high basal level production of darobactin (~4.7 µg/mL) even in the absence of IPTG (Fig. S3A). We

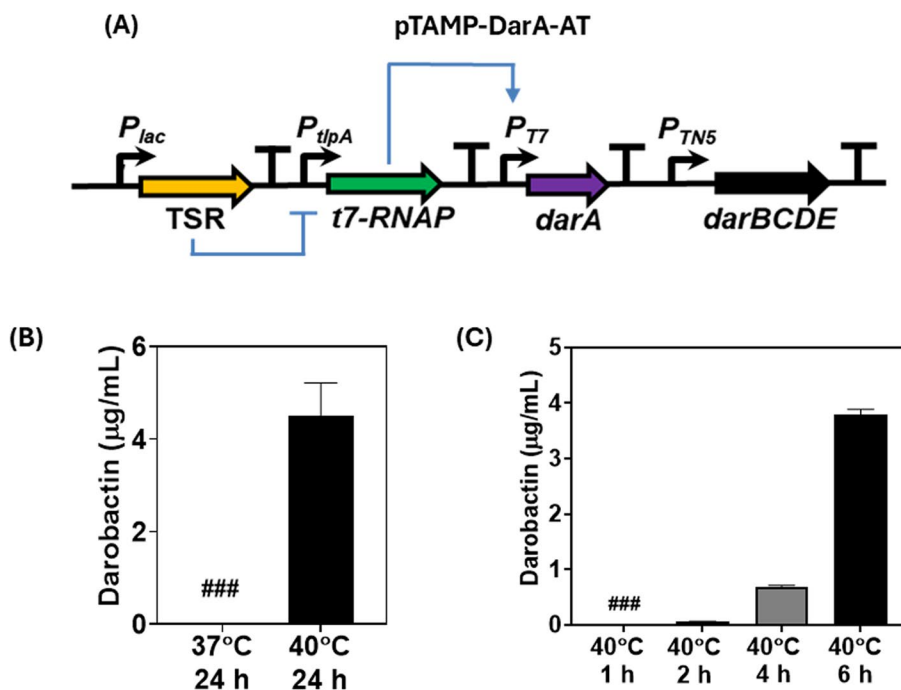


**Fig. 3** Testing the thermo-amplifier genetic circuit design in terms of darobactin production. **A** Schematic representation of the pTAMP-DarA-AT genetic circuit. The TSR represses the *t7-RNAP* gene at incubation temperatures < 37 °C, beyond which the TSR de-repression leads to *t7-RNAP* expression and  $P_{T7}$  promoter based darobactin production **(B)** Darobactin concentration in the liquid medium (µg/mL) for the pTAMP-DarA-AT construct in *E. coli* Nissle 1917 (EcN) after 24 h of incubation at 37 °C and 40 °C respectively. The error bars represent standard deviation based on three independent measurements. (###) represents darobactin concentrations lower than the Limit of Detection (LOD) by ESI-MS **(C)** Darobactin concentration in the liquid medium (µg/mL) for the pTAMP-DarA-AT EcN strain after 1, 2, 4 and 6 h of incubation at 40 °C, respectively. Error bars represent standard deviation from three independent measurements. (###) represents darobactin concentrations lower than the LOD by ESI-MS

also wanted to verify whether the unmodified EcN strain was able to produce darobactin when transformed with the thermoresponsive pTlp-DarA-AT plasmid. Post 24 h incubation, the darobactin concentration in the liquid medium (FM) without antibiotic supplementation for the pTlp-DarA-AT EcN strain was found to be  $\sim 0.02$   $\mu\text{g}/\text{mL}$  and  $\sim 0.07$   $\mu\text{g}/\text{mL}$  at 37 °C and 40 °C, respectively (Fig. S3B). This showed that the darobactin concentrations from EcN are very similar to that of the ClearColi strain, with an overall fold change of  $\sim 3\times$  at higher temperature (40 °C). Both these experiments validated that EcN was a suitable microbial chassis for constructing and testing the thermo-amplifier circuit.

Our key hypothesis was that post thermal induction (40 °C), the thermo-amplifier circuit should be able to offer higher levels of darobactin production, while showing minimal darobactin expression at physiological temperature (37 °C). Surprisingly, when the thermo-amplifier circuit was constructed in a plasmid, pTAMP-DarA-AT and tested in EcN, drastic improvement in the darobactin concentration (liquid medium) was observed at 40 °C ( $\sim 4.5$   $\mu\text{g}/\text{mL}$ ), while its presence was below the detection limit of 0.01  $\mu\text{g}/\text{mL}$  at 37 °C after 24 h incubation in FM (Fig. 3B). It is to be also noted that the darobactin concentration achieved with the pTAMP-DarA-AT EcN strain was  $\sim 1.6\times$ -fold higher than that obtained by the pNOSO-darABCDE ClearColi strain post-IPTG induction. In addition to darobactin production, we also wanted to assess whether the *txe-axe* TA module could mediate recombinant plasmid retention over several bacterial generations without external antibiotic supplementation. To do so, the pTAMP-DarA-AT EcN strain was cultivated for  $\sim 50$  consecutive generations in FM at 40 °C over a period of 5 days both with and without ampicillin supplementation (100  $\mu\text{g}/\text{mL}$ ). qPCR analysis of bacterial populations after 10 and 50 generations revealed no significant difference between the mean  $\Delta\text{Cq}$  fold change for the samples cultivated without antibiotic supplementation when compared to the antibiotic supplemented samples (Fig. S4). This suggested that the *txe-axe* TA system ensured that the microbial chassis retained the plasmid at similar copy numbers even after  $\sim 50$  generations of cell division in the absence of external selection pressure.

Since darobactin is responsible for the growth inhibition of Gram-negative bacteria, including *E. coli*, the effect of its overproduction in the EcN strain in terms of the bacterial growth kinetics needed to be tested. While the growth rate of the pTAMP-DarA-AT EcN strain was slightly reduced compared to the pTlp-DarA-AT EcN and wild type EcN strains at both 37 °C (Fig. S5A) and 40 °C (Fig. S5B) incubation temperatures, there was no significant difference between the lag phase as well as the

overall time required to reach maximal cell density for the strains. The growth curves also showed that all the strains had an exponential increase in their cell density up to 6 h, corresponding to their log phase beyond which slower growth rates were observed. This motivated us to determine whether thermal induction for shorter periods of time could produce detectable levels of darobactin in the liquid medium. Following this, we cultivated the pTAMP-DarA-AT EcN strain in FM for 1, 2, 4 and 6 h (periods corresponding to the log phase) at both the incubation temperatures of 37 °C and 40 °C. None of the bacterial samples incubated at 37 °C showed detectable levels of darobactin in the liquid medium. However, for the bacterial samples incubated at 40 °C, detectable levels of darobactin could be observed beyond 2 h incubation ( $\sim 0.06$   $\mu\text{g}/\text{mL}$ ), with darobactin concentrations reaching  $\sim 0.7$   $\mu\text{g}/\text{mL}$  and  $\sim 3.8$   $\mu\text{g}/\text{mL}$  upon 4 h and 6 h incubation, respectively (Fig. 3C). High darobactin levels in the liquid medium after 6 h incubation ascertained that the majority of darobactin was produced during the exponential growth phase of the recombinant strain, beyond which both the darobactin concentration and bacterial growth rate underwent gradual stagnation.

#### Analyzing the impact of shorter thermal induction periods on thermo-amplifier strain

To gain a better understanding, we conducted rt-PCR analysis for the *t7-RNAP* and *darA* genes of the pTAMP-DarA-AT EcN strain, post-incubation at 37 °C and 40 °C for 6 h. rt-PCR analysis revealed that the gene expression levels of *t7-RNAP* and *darA* were  $\sim 9$  and  $\sim 19\times$  fold higher at 40 °C than at 37 °C, respectively (Fig. 4A and B). In comparison, no significant upregulation in the  $P_{tlpA}$  promoter driven *darA* gene expression could be observed for the pTlp-DarA-AT EcN strain at 40 °C ( $11.6 \pm 0.3$  cycles) compared to 37 °C ( $11.5 \pm 1.7$  cycles) after 6 h incubation in FM (Fig. S6). This could explain the overall low darobactin concentration observed for the  $P_{tlpA}$  promoter-driven darobactin production by the pTlp-DarA-AT EcN strain after thermal induction. Furthermore, the quantification cycle (Cq) value of *darA* gene at 40 °C for the pTAMP-DarA-AT construct (EcN) was  $8.1 \pm 1.2$  cycles, which formed the logical basis for obtaining a higher darobactin concentration compared to the pTlp-DarA-AT construct (EcN) after a 6 h incubation period. This analysis suggested that the lower production levels of pTlp-DarA are due to the producer strains' inability to effectively transcribe the gene rather than the toxicity of mature darobactin. This could be due to one or more of the variety of mechanisms involving transcription factors and the RNA Polymerase that restrict transcription initiation [50], elongation [51], or termination [52]. Such transcriptional restrictions might originate from

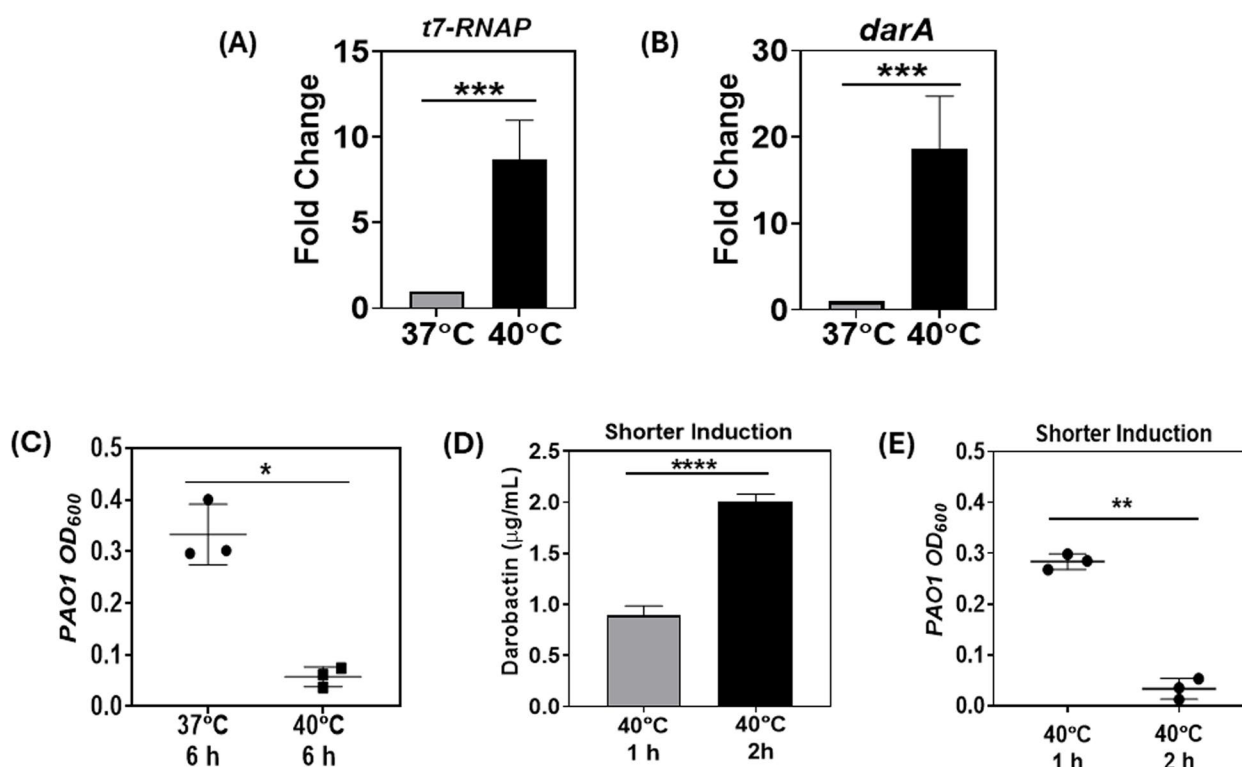


**Fig. 4** Effect of shorter periods of thermal induction on darobactin production. **A** Fold change in *t7-RNAP* gene expression driven by the  $P_{t7}$  promoter of pTAMP-DarA-AT construct in EcN at 37 °C and 40 °C after 6 h incubation in FM (without antibiotic supplementation). The error bars represent standard deviation based on six independent measurements (\*\* $p=0.0004$  as calculated by paired t-test) **B** Fold change in *darA* gene expression driven by the  $P_{t7}$  promoter of pTAMP-DarA-AT construct in EcN at 37 °C and 40 °C after 6 h incubation in FM (without antibiotic supplementation). The error bars represent standard deviation based on six independent measurements (\*\* $p=0.0009$  as calculated by paired t-test) **C** End-point absorbance ( $OD_{600}$ ) of *P. aeruginosa* PAO1 after 18 h incubation at 37 °C in filter-sterilized FM previously sustaining the growth of pTAMP-DarA-AT EcN strain. The FM collected from the 40 °C incubated samples demonstrate significant growth inhibition of *P. aeruginosa* PAO1. The error bars represent standard deviation based on three independent measurements (\* $p=0.0253$  as calculated by paired t-test) **D** Darobactin concentration in the liquid medium ( $\mu\text{g/mL}$ ) for the pTAMP-DarA-AT EcN strain grown in FM (without antibiotic supplementation) after 1 h and 2 h of shorter thermal induction (40 °C), followed by an additional 5 h and 4 h of incubation at 37 °C, respectively. The error bars represent standard deviation based on three independent measurements (\*\*\*\* $p<0.0001$  as calculated by paired t-test) **E** End-point absorbance ( $OD_{600}$ ) of *P. aeruginosa* PAO1 after 18 h incubation at 37 °C in filter-sterilized FM previously sustaining the growth of pTAMP-DarA-AT EcN strain. The FM collected from the 2 h thermally induced (40 °C) samples followed by an additional incubation at 37 °C for 4 h demonstrate significant growth inhibition of *P. aeruginosa* PAO1. The error bars represent standard deviation based on three independent measurements (\*\* $p=0.0014$  as calculated by paired t-test)

some unknown defense mechanism that prevent *E. coli* from expressing potentially toxic genes. Further in-depth investigations would be required to validate this hypothesis and unravel underlying mechanisms. Nevertheless, the limiting mechanism doesn't seem to affect transcription driven by the phage-derived T7-RNAP, possibly due to its partial orthogonality to host transcription factors.

Next, we determined whether the high levels of darobactin produced by the thermo-amplifier genetic circuit imparted antimicrobial activity against Gram-negative pathogens. We selected the commonly used laboratory strain, *P. aeruginosa* PAO1, as the indicator pathogen for our darobactin-based antimicrobial screening assays. Although *P. aeruginosa* is not a common enteric

pathogen, it has been reported to colonize the gastrointestinal tract and cause gut-derived sepsis, Shanghai fever, and severe respiratory infections, especially in infants and immunocompromised patients [42]. MIC experiments with pure darobactin revealed that concentrations above  $\sim 2 \mu\text{g/mL}$  could inhibit the growth of *P. aeruginosa* PAO1 in FM-based liquid cultures (Fig. S7), in accordance with previous studies [9]. Encouraged by these results, we tested whether the darobactin produced by the pTAMP-DarA-AT EcN strain could exert an antimicrobial activity against *P. aeruginosa* PAO1. Filter-sterilized supernatants collected from the pTAMP-DarA-AT EcN cultures after 6 h incubation at 37 °C and 40 °C, were inoculated with the *P. aeruginosa*

PAO1 strain. Post overnight incubation, only the bacterial supernatants collected from the 40 °C incubated pTAMP-Dar-AT EcN cultures inhibited the growth of *P. aeruginosa* PAO1. In contrast, the bacterial supernatants collected from their counterparts incubated at 37 °C failed to inhibit the growth of *P. aeruginosa* PAO1 (Fig. 4C). Although this was an interesting observation, thermal activation by high fever (>39 °C) or focused ultrasound cannot be expected to last for 6 h. For instance, high fever triggered by bacterial pyrogens either do not last longer than a couple hours [53] or are brought down by medication [54]. Therefore, thermal induction for the darobactin production cascade for a prolonged period of 6 h might not be most suitable for treating pathogen. Since the T7-RNAP produced by the thermo-amplifier circuit via thermal induction should remain active even after the temperature is lowered, we expected darobactin production to be sustained for longer. Therefore, we decided to test the minimal thermal induction threshold that would be suitable for both activation and sustained production of darobactin from the recombinant EcN strain. For that, we subjected the pTAMP-DarA-AT EcN strain to thermal induction at 40 °C for a 1 h and 2 h period, and then lowered the temperature to 37 °C for the following 5 h and 4 h, respectively. After the 6 h incubation period, ~0.9 µg/mL and ~2 µg/mL of darobactin could be detected in the liquid medium for the cultures subjected to the short thermal induction periods of 1 h and 2 h, respectively (Fig. 4D). The higher darobactin concentration observed for the 2 h induced samples were also able to effectively inhibit the growth of *P. aeruginosa* PAO1 (Fig. 4E), whereas the 1 h induced samples did not demonstrate significant antimicrobial activity. Considering the results in Fig. 3C, which show that 2 h of thermal induction doesn't produce more than 0.6 µg/mL, the results of Fig. 4E suggests that the darobactin production is sustained beyond the duration of thermal induction. Thus, thermal induction at 40 °C for 2 h followed by an additional 4 h incubation at 37 °C was sufficient to activate and sustain darobactin production from the pTAMP-DarA-AT EcN strain to inhibit *P. aeruginosa* PAO1 growth.

#### Testing the performance of thermo-amplifier strain under harsh growth conditions

When considering potential applicability in the gastrointestinal tract, the recombinant pTAMP-DarA-AT EcN strain must be able to perform under conditions of nutrient limitation and the presence of bile acids [55]. Therefore, we tested our engineered EcN strains in a nutrient-limited medium resembling the gut luminal content [56]. The pTAMP-DarA-AT EcN strain was inoculated in M9

Minimal Media and subjected to thermal induction for 2 h at 40 °C, with an additional incubation of 4 h at 37 °C. However, this medium was not able to support the growth of sufficient biomass to generate pathogen-inhibiting quantities of darobactin concentration (<0.1 µg/mL). Thus, we mimicked the high-biomass delivery modality used for probiotics and living therapeutics by first growing the bacteria to a sufficient biomass in FM medium at 30 °C (OFF state), then testing their darobactin production capacity in M9 Minimal Medium at 40 °C (ON state). The harvested biomass from FM medium was re-suspended in M9 Minimal Media and subjected to thermal induction at 40 °C for 2 h, followed by an additional incubation of 4 h at 37 °C. Post thermal induction, darobactin concentration in the supernatants reached up to ~1.8 µg/mL, whereas the control samples incubated at 37 °C for 6 h produced only ~0.3 µg/mL of darobactin (Fig. 5A). Pre-cultivating the bacterial biomass for 24 h may have resulted in the basal level expression of T7-RNAP, leading to the leaky darobactin production from the resuspended samples incubated at 37 °C. However, the ~6×fold higher concentration of darobactin in the supernatants collected from the thermally induced bacterial samples demonstrated significant growth inhibition of *P. aeruginosa* PAO1 compared to the control samples (Fig. 5B). Finally, we tested the darobactin production capacity of the pTAMP-DarA-AT EcN strain in the presence of bile stress, which is known to promote antibiotic resistance [57] and biofilm formation [58] in *P. aeruginosa* PAO1. For this, the pre-cultivated biomass of the pTAMP-DarA-AT EcN strain was resuspended in M9 Minimal Media supplemented with 0.3% (w/v) Bovine Bile, and then subjected to a 2 h thermal induction at 40 °C followed by an additional incubation at 37 °C for 4 h. Upon further analysis, ~2.2 µg/mL of darobactin could be observed in the supernatants of the thermally induced bacterial samples, whereas ~0.5 µg/mL of darobactin could be detected in the supernatants of the control samples incubated at 37 °C (Fig. 5C). The similar darobactin concentration fold change (~5x) suggested that bile stress did not significantly affect the darobactin production capacity of the thermo-amplifier EcN strain. In addition, the supernatants of the thermally induced bacterial samples also showed significant growth inhibition of *P. aeruginosa* PAO1 compared to the control samples suggesting that bile supplementation did not reduce the antimicrobial activity of darobactin (Fig. 5D). These experiments confirmed that the thermo-amplifier EcN strain could sustain darobactin production in the presence of stress factors, such as bile and nutrient limitations.

#### Discussions

In this study, we have demonstrated the challenges in regulating the production of an enzymatically synthesized novel antibiotic and developed a solution to overcome

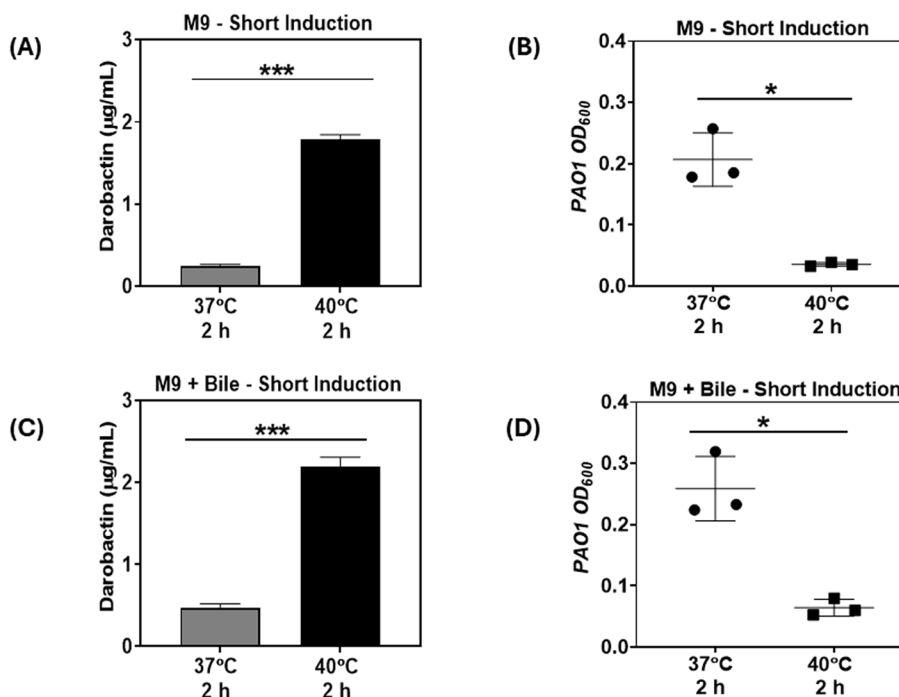


**Fig. 5** Role of harsh conditions in influencing darobactin production and antimicrobial activity. **A** Darobactin concentration ( $\mu\text{g/mL}$ ) in M9 Minimal Media sustaining the pre-cultivated biomass of pTAMP-DarA-AT EcN strain (no antibiotic supplementation) after 2 h incubation at 37 °C and 40 °C (thermal induction), followed by an additional 4 h incubation at 37 °C. The error bars represent standard deviation based on three independent measurements ( $***p=0.0004$  as calculated by paired t-test) **(B)** End-point absorbance ( $\text{OD}_{600}$ ) of *P. aeruginosa* PAO1 after 18 h incubation at 37 °C in filter-sterilized M9 Minimal Media containing the pTAMP-DarA-AT EcN strain. The samples subjected to thermal induction (40 °C) for 2 h followed by an additional incubation at 37 °C for 4 h demonstrate significant growth inhibition of *P. aeruginosa* PAO1. The error bars represent standard deviation based on three independent measurements ( $*p=0.0234$  as calculated by paired t-test) **(C)** Darobactin concentration ( $\mu\text{g/mL}$ ) in M9 Minimal Media supplemented with 0.3% (w/v) Bovine Bile sustaining the pre-cultivated biomass of pTAMP-DarA-AT EcN strain (no antibiotic supplementation) after 2 h incubation at 37 °C and 40 °C (thermal induction), followed by an additional 4 h incubation at 37 °C. The error bars represent standard deviation based on three independent measurements ( $***p=0.0005$  as calculated by paired t-test) **(D)** End-point absorbance ( $\text{OD}_{600}$ ) of *P. aeruginosa* PAO1 after 18 h incubation at 37 °C in filter-sterilized M9 Minimal Media supplemented with 0.3% (w/v) Bovine Bile, containing the pTAMP-DarA-AT EcN strain. The samples subjected to thermal induction (40 °C) for 2 h followed by an additional incubation at 37 °C for 4 h demonstrate significant growth inhibition of *P. aeruginosa* PAO1. The error bars represent standard deviation based on three independent measurements ( $*p=0.0328$  as calculated by paired t-test)

those challenges. Specifically, we show how one inducible system (IPTG) results in high production of darobactin but also suffers from significant basal level expression. This basal level expression can occur due to the affinity of the lacI repressor protein to related auto-inducer molecules, like lactose (disaccharide) and galactose (monosaccharide) present in the growth media as reported previously [59]. Such cross-reactivity to simple carbohydrates cannot be reasonably avoided when pathogen inhibition is to be tested under therapeutically relevant conditions. On the other hand, such cross-reactivity does not occur in the TlpA-based thermoresponsive genetic switch [60] but its transcriptional limitations can restrict heterologous protein production in the microbial chassis and reduce their application potential. This was observed in our case, where the standard thermal induction circuit could not reach the expected darobactin production levels in the liquid medium that was observed for the IPTG

inducible system. By combining components from both systems, we developed a thermo-amplifier circuit that achieved undetectable levels of leaky production and high levels of thermally induced darobactin production in the growth medium. This was done by exploiting the strong transcriptional rate of the T7 promoter as previously reported for the opto-T7-RNAP and related systems [61, 62]. The orthogonality of the T7 RNA Polymerase system also seems to overcome limitations imposed by the host transcription machinery, which in the case of  $P_{tlpA}$ -driven darobactin production resulted in very low yields. Thus, for the first time, we have demonstrated the advantages of combining thermo-genetics with the prolific strength and orthogonality of the T7-RNAP-T7 promoter combination and demonstrated the superior performance of this circuit for darobactin production. Furthermore, a favorable consequence of the thermo-amplifier circuit design is the sustained production of darobactin even after only

a short duration (2 h) of thermal induction. Such short durations of raised body temperature can more conceivably be achieved by high fever or focused ultrasound. This performance was retained even in the presence of bile salts and under low-nutrient conditions, which better mimic the environment in the intestines [55]. Follow-up studies will establish co-culture and biofilm models to investigate the direct pathogen killing capabilities of the engineered *E. coli* strain under physiologically relevant conditions. Previous reports have shown considerable improvements in engineering *E. coli*-based strains, to sense and eliminate *P. aeruginosa* PAO1, both under *in-vitro* [63] and *in-vivo* [64] conditions. The engineered strains could detect low levels of the quorum sensing molecule, N-acyl homoserine lactone (3OC<sub>12</sub>-HSL) and undergo auto-lysis to release anti-*P. aeruginosa* toxin, pyocin S5 and reduce gut infections in animal models. As pointed out by Hwang and co-workers engineered EcN strains could colonize the mice intestine for a period of 3 weeks, which provided an extended temporal window to facilitate complete pathogen clearance. Furthermore, EcN strains have been engineered to produce surface-displayed adhesins or curli fiber matrices that improve their retention and local density in the intestines for drug delivery [65, 66]. These promising engineering strategies can be combined with our thermo-amplifier darobactin circuit to improve its applicability in the body.

In the current study, all these components are encoded in a single plasmid for ease of manipulation and testing across different *E. coli* strains. The plasmid hosts a toxin-antitoxin system that ensures retention and desired darobactin production levels without antibiotic supplementation. Nevertheless, the presence of genes encoding for darobactin exporter enzymes in the recombinant plasmid also increased the darobactin tolerance of the EcN as shown by the MIC values (> 16 µg/mL compared to 1.6 µg/mL of wild type EcN) without affecting the growth, which is consistent with the results previously observed for a standard *E. coli* BL21 DE3 strain [9]. This raises concerns regarding horizontal transfer of the plasmids leading to darobactin resistance in other microbes. In follow-up studies, we will explore two strategies to mitigate this potential risk – (i) encode the darBCD cluster in the genome, and (ii) encapsulate the bacteria in polymeric matrices that prevent horizontal gene transfer [67]. The second approach, based on engineered living materials, also offers additional benefits conferred by the material component such as protection of the bacteria in the body and their physical biocontainment [22]. This strategy is being increasingly explored to overcome challenges of balancing efficacy and biosafety in engineered living therapeutics [20, 68].

While the current study has demonstrated the effectiveness of the darobactin-producing thermo-amplifier circuit using a model pathogen, *P. aeruginosa* PAO1, this drug has broad spectrum antimicrobial activity against several Gram-negative pathogens [5, 9]. The applicability of this system to treat other infections caused by pathogens like *Klebsiella*, *Salmonella*, *Shigella*, etc. is of great interest for future studies. Beyond darobactin, the thermo-amplifier circuit could also be adapted to achieve highly regulated production of other enzymatically synthesized therapeutic compounds. For example, it can be applied to numerous bioactive RiPPs like darobactin whose BGCs have been recently elucidated and reconstructed for heterologous expression in *E. coli* [69]. Finally, beyond thermal induction, the amplification strategy using the T7 RNA Polymerase and its cognate promoter could be adapted for other inducible systems that suffer from poor performance either due to high leaky expression, low post-induction expression levels, or interference from host transcriptional machinery.

## Conclusions

Living therapeutics represents an exciting frontier for realizing long-term, low-cost and controlled drug release within the body. However, creating leak-free and rapidly responsive genetic switches to control drug release remains a major challenge hindering the field, especially for drugs that require post-translational modification and are toxic to the production host. In this study, we have presented a novel strategy to achieve stringent genetic control over the production and release of a complex post-translationally modified peptide drug, darobactin, using probiotic bacteria. While well-known IPTG- and thermo-responsive genetic switches achieved either leaky or insufficient production, the careful combination of parts from both switches resulted in a thermo-amplifier circuit that overcame both issues. The production and release of darobactin at pathogen-inhibitory levels using an antibiotic-free plasmid retention system under physiologically relevant conditions highlights the possibility of developing such probiotics as delivery vehicles for drugs that are challenging to mass-produce at low cost.

## Supplementary Information

The online version contains supplementary material available at <https://doi.org/10.1186/s13036-024-00463-y>.

Additional file 1: Fig. S1. Comparative mCherry production by the pNOSO-mCherry and pUC-Tlp-mCherry plasmids in ClearColi BL21 DE3. Fig. S2. Comparative analysis of biomass and darobactin production by the pNOSO-darABCDE and pT7-DarA plasmids in ClearColi BL21 DE3. Fig. S3. Comparative analysis of darobactin production by the pNOSO-darABCDE and pTlp-DarA-AT plasmids in EcN-T7 and EcN strains respectively. Fig. S4. qPCR analysis-based assessment of pTAMP-DarA-AT recombinant plasmid retention in EcN with and without antibiotic supplementation. Fig. S5.

Growth kinetics of the engineered strains at 37 °C and 40 °C. Fig. S6. *darA* gene expression level by the pTlp-DarA-AT plasmid. Fig. S7. Minimum Inhibitory Concentration (MIC) of darobactin for *Pseudomonas aeruginosa* PAO1 strain. Fig. S8 & Fig. S9. Sequence annotated maps of pTlp-DarA-AT and pTAMP-DarA-AT recombinant plasmids. Table S1. Nucleotide sequences of genetic modules. Table S2. Primer sequences for qRT-PCR and qPCR analysis.

### Acknowledgements

We would like to thank Mikhail Shapiro for the pTlpA39-mWasabi plasmid (Addgene #86116), Chris Barnes for the pUC-GFP AT plasmid (Addgene #133306) and Paul Freemont for the mBP-T7RNAP plasmid (Addgene #74096). We thank Nicole Frankenberg-Dinke for providing us with the EcN-T7 strain (DSMZ 115365). We thank Sanjana Balaji Kuttae for her help with the construction of the recombinant plasmids. We thank Ha Rimbach-Nguyen for assisting with the ESI-MS analysis of darobactin concentration in bacterial supernatants. All the schematic figures were generated using Biorender.

### Authors' contributions

S.D. designed and constructed the plasmids, performed experiments, and analyzed the data. C.E.S. provided the purified darobactin standard. C.F.S. and A.M.K. performed the quantitative estimation of darobactin in the extracellular media. S.S. and R. M. conceived and oversaw the overall project. S.D. and S.S. wrote the manuscript. C.E.S. and R.M. revised the manuscript. All authors read and approved the manuscript.

### Funding

Open Access funding enabled and organized by Projekt DEAL. This work was supported by the Leibniz Science Campus on Living Therapeutic Materials [LifeMat].

### Data availability

The authors declare that the data supporting the findings of this study are available within the paper and its Supplementary Information files. Should any raw data files be needed in another format they are available from the corresponding author upon reasonable request. Data are located in controlled access data storage at the INM—Leibniz Institute for New Materials.

### Declarations

#### Ethics approval and consent to participate

Not applicable.

#### Consent for publication

Not applicable.

#### Competing interests

R.M. and C.E.S. are inventors of patent application WO2022175443A1, titled "Novel darobactin derivatives".

#### Author details

<sup>1</sup>INM - Leibniz Institute for New Materials, Campus D2 2, 66123 Saarbrücken, Germany. <sup>2</sup>Microbial Natural Products, Helmholtz Institute for Pharmaceutical Research Saarland (HIPS), Helmholtz Centre for Infection Research (HZI), Saarbrücken, Germany. <sup>3</sup>Department of Pharmacy, Saarland University, Campus Building E8.1, 66123 Saarbrücken, Germany. <sup>4</sup>German Centre for Infection Research (DZIF), Partner Site Hannover, Brunswick, Germany.

Received: 2 September 2024 Accepted: 30 October 2024

Published online: 12 November 2024

### References

- Wang L, Wang N, Zhang W, Cheng X, Yan Z, Shao G, Wang X, Wang R, Fu C. Therapeutic peptides: current applications and future directions. *Signal Transduct Target Ther*. 2022;7(1):48.
- Pereira AJ, de Campos LJ, Xing H, Conda-Sheridan M. Peptide-based therapeutics: challenges and solutions. *Med Chem Res*. 2024;27:1–6.
- Fetse J, Kandel S, Mamani UF, Cheng K. Recent advances in the development of therapeutic peptides. *Trends Pharmacol Sci*. 2023;44(7):425–41.
- Craik DJ, Fairlie DP, Liras S, Price D. The future of peptide-based drugs. *Chem Biol Drug Des*. 2013;81(1):136–47.
- Imai Y, Meyer KJ, Iinishi A, Favre-Godal Q, Green R, Manuse S, Caboni M, Mori M, Niles S, Ghiglieri M, Honrao C. A new antibiotic selectively kills Gram-negative pathogens. *Nature*. 2019;576(7787):459–64.
- Seyfert CE, Porten C, Yuan B, Deckarm S, Panter F, Bader CD, Coetzee J, Deschner F, Tehrani KH, Higgins PG, Seifert H. Darobactins exhibiting superior antibiotic activity by Cryo-EM structure guided biosynthetic engineering. *Angew Chem Int Ed*. 2023;62(2):e202214094.
- Li X, Ma S, Zhang Q. Chemical synthesis and biosynthesis of darobactin. *Tetrahedron Lett*. 2023;116:154337.
- Wuisan ZG, Kresna ID, Böhringer N, Lewis K, Schäberle TF. Optimization of heterologous Darobactin A expression and identification of the minimal biosynthetic gene cluster. *Metab Eng*. 2021;1(66):123–36.
- Groß S, Panter F, Pogorevc D, Seyfert CE, Deckarm S, Bader CD, Herrmann J, Müller R. Improved broad-spectrum antibiotics against Gram-negative pathogens via darobactin biosynthetic pathway engineering. *Chem Sci*. 2021;12(35):11882–93.
- Pedroli DB, Ribeiro NV, Squizato PN, de Jesus VN, Cozetto DA, Tuma RB, Gracindo A, Cesar MB, Freire PJ, da Costa AF, Lins MR. Engineering microbial living therapeutics: the synthetic biology toolbox. *Trends Biotechnol*. 2019;37(1):100–15.
- Charbonneau MR, Isabella VM, Li N, Kurtz CB. Developing a new class of engineered live bacterial therapeutics to treat human diseases. *Nat Commun*. 2020;11(1):1738.
- Liu Y, Feng J, Pan H, Zhang X, Zhang Y. Genetically engineered bacterium: Principles, practices, and prospects. *Front Microbiol*. 2022;13:997587.
- Kelly VW, Liang BK, Sirk SJ. Living therapeutics: the next frontier of precision medicine. *ACS Synth Biol*. 2020;9(12):3184–201.
- Beceiro A, Tomás M, Bou G. Antimicrobial resistance and virulence: a successful or deleterious association in the bacterial world? *Clin Microbiol Rev*. 2013;26(2):185–230.
- Isabella VM, Ha BN, Castillo MJ, Lubkowicz DJ, Rowe SE, Millet YA, Anderson CL, Li N, Fisher AB, West KA, Reeder PJ. Development of a synthetic live bacterial therapeutic for the human metabolic disease phenylketonuria. *Nat Biotechnol*. 2018;36(9):857–64.
- Medina C, Camacho EM, Flores A, Mesa-Pereira B, Santero E. Improved expression systems for regulated expression in *Salmonella* infecting eukaryotic cells. *PLoS ONE*. 2011;6(8):e23055.
- Liu X, Wu M, Wang M, Duan Y, Phan C, Qi G, Tang G, Liu B. Metabolically engineered bacteria as light-controlled living therapeutics for anti-angiogenesis tumor therapy. *Mater Horiz*. 2021;8(5):1454–60.
- Piraner DI, Abedi MH, Moser BA, Lee-Gosselin A, Shapiro MG. Tunable thermal bioswitches for in vivo control of microbial therapeutics. *Nat Chem Biol*. 2017;13(1):75–80.
- Maresca D, Lakshmanan A, Abedi M, Bar-Zion A, Farhadi A, Lu GJ, Szabrowski JO, Wu D, Yoo S, Shapiro MG. Biomolecular ultrasound and sonogenetics. *Annu Rev Chem Biomol Eng*. 2018;9(1):229–52.
- Omer R, Mohsin MZ, Mohsin A, Mushtaq BS, Huang X, Guo M, Zhuang Y, Huang J. Engineered bacteria-based living materials for biotherapeutic applications. *Front Bioeng Biotechnol*. 2022;28(10):870675.
- Rodrigo-Navarro A, Sankaran S, Dalby MJ, del Campo A, Salm-eron-Sanchez M. Engineered living biomaterials. *Nat Rev Mater*. 2021;6(12):1175–90.
- Dey S, Sankaran S. Engineered bacterial therapeutics with material solutions. *Trends Biotechnol*. 2024. <https://doi.org/10.1016/j.tibtech.2024.06.011>.
- Zhou Y, Han Y. Engineered bacteria as drug delivery vehicles: principles and prospects. *Eng Microbiol*. 2022;2(3):100034.
- Kan A, Gelfat I, Emani S, Praveschotinunt P, Joshi NS. Plasmid vectors for in vivo selection-free use with the probiotic *E. coli* Nissle 1917. *ACS Synthetic Biol*. 2020;10(1):94–106.
- Abedi MH, Yao MS, Mittelstein DR, Bar-Zion A, Swift MB, Lee-Gosselin A, Barturen-Larrea P, Buss MT, Shapiro MG. Ultrasound-controllable

- engineered bacteria for cancer immunotherapy. *Nat Commun.* 2022;13(1):1585.
26. Li L, Pan H, Pang G, Lang H, Shen Y, Sun T, Zhang Y, Liu J, Chang J, Kang J, Zheng H. Precise thermal regulation of engineered bacteria secretion for breast cancer treatment in vivo. *ACS Synth Biol.* 2022;11(3):1167–77.
  27. Sankaran S, Becker J, Wittmann C, Del Campo A. Optoregulated drug release from an engineered living material: self-replenishing drug depots for long-term, light-regulated delivery. *Small.* 2019;15(5):1804717.
  28. Sugianto W, Altin-Yavuzarslan G, Tickman BI, Kiattisewee C, Yuan SF, Brooks SM, Wong J, Alper HS, Nelson A, Carothers JM. Gene expression dynamics in input-responsive engineered living materials programmed for bioproduction. *Materials Today Bio.* 2023;1(20):100677.
  29. Seyfert CE, Müller AV, Walsh DJ, Birkelbach J, Kany AM, Porten C, Yuan B, Krug D, Herrmann J, Marlovits TC, Hirsch AK. New genetically engineered derivatives of antibacterial darobactins underpin their potential for antibiotic development. *J Med Chem.* 2023;66(23):16330–41.
  30. Škulj M, Okršlar V, Jalen Š, Jevševar S, Slanc P, Štrukelj B, Menart V. Improved determination of plasmid copy number using quantitative real-time PCR for monitoring fermentation processes. *Microb Cell Fact.* 2008;7:1–2.
  31. Smati M, Clermont O, Le Gal F, Schichmanoff O, Jauréguy F, Eddi A, Denamur E, Picard B, Colville Group. Real-time PCR for quantitative analysis of human commensal *Escherichia coli* populations reveals a high frequency of subdominant phylogroups. *Applied and environmental microbiology.* 2013;79(16):5005–12.
  32. Nickerson KP, Faherty CS. Bile salt-induced biofilm formation in enteric pathogens: techniques for identification and quantification. *JoVE (Journal of Visualized Experiments).* 2018;135:e57322.
  33. Mamat U, Wilke K, Bramhill D, Schromm AB, Lindner B, Kohl TA, Corchero JL, Villaverde A, Schaffer L, Head SR, Souvignier C. Detoxifying *Escherichia coli* for endotoxin-free production of recombinant proteins. *Microb Cell Fact.* 2015;14:1–5.
  34. Dhakane P, Tadimarri VS, Sankaran S. Light-Regulated Pro-Angiogenic Engineered Living Materials. *Adv Func Mater.* 2023;33(31):2212695.
  35. Yanamandra AK, Bhusari S, Del Campo A, Sankaran S, Qu B. In vitro evaluation of immune responses to bacterial hydrogels for the development of living therapeutic materials. *Biomater Adv.* 2023;1(153):213554.
  36. Nguyen H, Made Kresna ID, Böhringer N, Ruel J, Mora ED, Kramer JC, Lewis K, Nicolet Y, Schäberle TF, Yokoyama K. Characterization of a radical SAM oxygenase for the ether crosslinking in darobactin biosynthesis. *J Am Chem Soc.* 2022;144(41):18876–86.
  37. Basaran S, Dey S, Bhusari S, Sankaran S, Kraus T. Plasmonic stimulation of gold nanorods for the photothermal control of engineered living materials. *Biomaterials Advances.* 2023;147:213332.
  38. Singha TK, Gulati P, Mohanty A, Khasa YP, Kapoor RK, Kumar S. Efficient genetic approaches for improvement of plasmid based expression of recombinant protein in *Escherichia coli*: A review. *Process Biochem.* 2017;55:17–31.
  39. Landry BP, Tabor JJ. Engineering diagnostic and therapeutic gut bacteria. In: *Bugs as drugs: therapeutic microbes for the prevention and treatment of disease.* 2018. p. 331–61.
  40. Aggarwal N, Breedon AM, Davis CM, Hwang IY, Chang MW. Engineering probiotics for therapeutic applications: recent examples and translational outlook. *Curr Opin Biotechnol.* 2020;65:171–9.
  41. Durmusoglu D, Al'Abri I, Li Z, Islam Williams T, Collins LB, Martínez JL, Crook N. Improving therapeutic protein secretion in the probiotic yeast *Saccharomyces boulardii* using a multifactorial engineering approach. *Microbial Cell Factories.* 2023;22(1):109.
  42. Hwang IY, Koh E, Wong A, March JC, Bentley WE, Lee YS, Chang MW. Engineered probiotic *Escherichia coli* can eliminate and prevent *Pseudomonas aeruginosa* gut infection in animal models. *Nat Commun.* 2017;8(1):15028.
  43. Gurbatri CR, Lia I, Vincent R, Coker C, Castro S, Treuting PM, Hinchliffe TE, Arpaia N, Danino T. Engineered probiotics for local tumor delivery of checkpoint blockade nanobodies. *Science translational medicine.* 2020;12(530):eaax0876.
  44. Grady R, Hayes F. Axe-Txe, a broad-spectrum proteic toxin–antitoxin system specified by a multidrug-resistant, clinical isolate of *Enterococcus faecium*. *Mol Microbiol.* 2003;47(5):1419–32.
  45. Halvorsen EM, Williams JJ, Bhimani AJ, Billings EA, Hergenrother PJ. Txe, an endoribonuclease of the enterococcal Axe-Txe toxin–antitoxin system, cleaves mRNA and inhibits protein synthesis. *Microbiology.* 2011;157(2):387–97.
  46. Fedorec AJ, Ozdemir T, Doshi A, Ho YK, Rosa L, Rutter J, Velazquez O, Pinheiro VB, Danino T, Barnes CP. Two new plasmid post-segregational killing mechanisms for the implementation of synthetic gene networks in *Escherichia coli*. *Iscience.* 2019;26(14):323–34.
  47. Harimoto T, Hahn J, Chen YY, Im J, Zhang J, Hou N, Li F, Coker C, Gray K, Harr N, Chowdhury S. A programmable encapsulation system improves delivery of therapeutic bacteria in mice. *Nat Biotechnol.* 2022;40(8):1259–69.
  48. Yu M, Hu S, Tang B, Yang H, Sun D. Engineering *Escherichia coli* Nissle 1917 as a microbial chassis for therapeutic and industrial applications. *Biotechnol Adv.* 2023;67:108202.
  49. Fiege K, Frankenberg-Dinkel N. Construction of a new T7 promoter compatible *Escherichia coli* Nissle 1917 strain for recombinant production of heme-dependent proteins. *Microb Cell Fact.* 2020;19(1):190.
  50. Engl C, Jovanovic G, Brackston RD, KottaLoizou I, Buck M. The route to transcription initiation determines the mode of transcriptional bursting in *E. coli*. *Nat Commun.* 2020;11(1):2422.
  51. Epshtein V, Toulmé F, Rahmouni AR, Borukhov S, Nudler E. Transcription through the roadblocks: the role of RNA polymerase cooperation. *EMBO J.* 2003;22(18):4719–27.
  52. Zhu C, Guo X, Dumas P, Takacs M, Abdelkareem MM, Vanden Broeck A, Saint-André C, Papai G, Crucifix C, Ortiz J, Weixlbaumer A. Transcription factors modulate RNA polymerase conformational equilibrium. *Nat Commun.* 2022;13(1):1546.
  53. Stokes WS, Marsman DS. Animal welfare considerations in biomedical research and testing. In: *Laboratory Animal Welfare* 2014 Jan 1 (pp. 115–140). Academic press.
  54. Perrott DA, Piira T, Goodenough B, Champion GD. Efficacy and safety of acetaminophen vs ibuprofen for treating children's pain or fever: a meta-analysis. *Arch Pediatr Adolesc Med.* 2004;158(6):521–6.
  55. De Paepe M, Gaboriau-Routhiau V, Rainteau D, Rakotobe S, Taddei F, Cerf-Bensussan N. Trade-off between bile resistance and nutritional competence drives *Escherichia coli* diversification in the mouse gut. *PLoS Genet.* 2011;7(6):e1002107.
  56. Ferraris RP, Yasharpour SA, Lloyd KC, Mirzayan RA, Diamond JM. Luminal glucose concentrations in the gut under normal conditions. *American Journal of Physiology-Gastrointestinal and Liver Physiology.* 1990;259(5):G822–37.
  57. Reen FJ, Flynn S, Woods DF, Dunphy N, Chróinin MN, Mullane D, Stick S, Adams C, O'Gara F. Bile signalling promotes chronic respiratory infections and antibiotic tolerance. *Sci Rep.* 2016;6(1):29768.
  58. Flynn S, Reen FJ, O'Gara F. Exposure to bile leads to the emergence of adaptive signaling variants in the opportunistic pathogen *Pseudomonas aeruginosa*. *Front Microbiol.* 2019;29(10):2013.
  59. Xu J, Banerjee A, Pan SH, Li ZJ. Galactose can be an inducer for production of therapeutic proteins by auto-induction using *E. coli* BL21 strains. *Protein Expr Purif.* 2012;83(1):30–6.
  60. Piraner DI, Farhadi A, Davis HC, Wu D, Maresca D, Szablowski JO, Shapiro MG. Going deeper: biomolecular tools for acoustic and magnetic imaging and control of cellular function. *Biochemistry.* 2017;56(39):5202–9.
  61. Raghavan AR, Salim K, Yadav VG. Optogenetic control of heterologous metabolism in *E. coli*. *ACS synthetic biology.* 2020;9(9):2291–300.
  62. Fernandez-Rodríguez J, Moser F, Song M, Voigt CA. Engineering RGB color vision into *Escherichia coli*. *Nat Chem Biol.* 2017;13(7):706–8.
  63. Saeidi N, Wong CK, Lo TM, Nguyen HX, Ling H, Leong SS, Poh CL, Chang MW. Engineering microbes to sense and eradicate *Pseudomonas aeruginosa*, a human pathogen. *Mol Syst Biol.* 2011;7(1):521.
  64. Hwang IY, Lee HL, Huang JG, Lim YY, Yew WS, Lee YS, Chang MW. Engineering microbes for targeted strikes against human pathogens. *Cell Mol Life Sci.* 2018;75:2719–33.
  65. Cui M, Sun T, Li S, Pan H, Liu J, Zhang X, Li L, Li S, Wei C, Yu C, Yang C. NIR light-responsive bacteria with live bio-glue coatings for precise colonization in the gut. *Cell Rep.* 2021;36(11):109690.
  66. Praveschotinunt P, Duraj-Thatte AM, Gelfat I, Bahl F, Chou DB, Joshi NS. Engineered *E. coli* Nissle 1917 for the delivery of matrix-tethered therapeutic domains to the gut. *Nature communications.* 2019;10(1):5580.

67. Tang TC, Tham E, Liu X, Yehl K, Rovner AJ, Yuk H, de la Fuente-Nunez C, Isaacs FJ, Zhao X, Lu TK. Hydrogel-based biocontainment of bacteria for continuous sensing and computation. *Nat Chem Biol.* 2021;17(6):724–31.
68. Dong X, Wu W, Pan P, Zhang XZ. Engineered living materials for advanced diseases therapy. *Adv Mater.* 2023;2304963. <https://doi.org/10.1002/adma.202304963>.
69. Zhong G, Wang ZJ, Yan F, Zhang Y, Huo L. Recent advances in discovery, bioengineering, and bioactivity-evaluation of ribosomally synthesized and post-translationally modified peptides. *ACS bio & med Chem Au.* 2022;3(1):1–31.

### **Publisher's Note**

Springer Nature remains neutral with regard to jurisdictional claims in published maps and institutional affiliations.